

# Chapter 1

## Introduction

### 1.1 History of Vacuum Microelectronics

Since the 1960s, there has been a substantial interest in field emitters and vacuum microelectronics that has been stimulated by the growth and evolution of solid-state technologies. That vacuum microelectronics should rival solid-state technology because vacuum, as a medium, offers unique and unsurpassed characteristics. For instance, the limiting carrier velocity in vacuum is the speed of light, which is far better than those in silicon or gallium arsenide. Similarly, carrier mobility in vacuum is virtually infinite, higher than in any semiconductor [1.1]. For the past decades, great improvements on semiconductor manufacturing technology gave a new life to vacuum electronics for the professional micro fabrication process to fabricate tiny vacuum devices. “Vacuum state” devices have a great deal of superior advantages as compared with solid-state devices, including fast carrier drift velocity, radiation hardness, and temperature insensitivity. For example, the saturation drift velocity is limited to less than  $3 \times 10^7$  cm/s in all semiconductor due to scattering mechanism whereas the saturation drift velocity in vacuum is limited theoretically to  $3 \times 10^8$  cm/s and practically to about  $6-9 \times 10^8$  cm/s [1.2]. Moreover, temporarily or permanently radiation effect is negligible in vacuum devices for no medium can be damaged. Additionally, the effect of temperature on performance is reduced in vacuum devices simply for no medium to cause the temperature effect in semiconductor, such as increased lattice scattering or bulk carrier generation/recombination. **Table 1-1** shows the comparison between vacuum microelectronic

and semiconductor devices.

Recent development in vacuum microelectronics started in 1928, when R. H. Fowler and L. W. Nordheim published the first theory of electron field emission from metals using quantum mechanics [1.3]. This theory is contrary to thermionic emission, which metals have to be heated so that some of the electrons in metal gain enough thermal energy to overcome the metal/vacuum barrier; according to the Fowler-Nordheim theory, an applied electric field of approximately  $10^3$  V/ $\mu\text{m}$  is needed for electrons to tunnel through the sufficiently narrow barrier [1.3]. To reach this high field at reasonable applied voltage, producing the field emitters into protruding objects is essential to take advantage of field enhancement. It was not until 1968 when C. A. Spindt came up with a fabrication method to create very small dimension metal cones that vacuum microelectronic triodes became possible (as shown in figure 1-1) [1.4]. From the late 1960s to the year 1990, Ivor Brodie, Henry F. Gray, and C. A. Spindt made many contributions to this field. Also, most of research was focused on the devices similar to the Spindt cathode during the past three decades.

In 1991, a group of research of the French company LETI CHEN reported a microtip display at the fourth International Vacuum Microelectronics Conference [1.5]. Their display was the first announcement of a practical vacuum microelectronic device. From then on, a great amount of researchers all over the world devoted themselves to this interesting, challenging, and inventive field. Part of the work focused on fabricating very small radius silicon tip by utilizing modern VLSI technology [1.6-1.7]. Some of them increased the emission current by coating different metals, such as W, Mo, Ta, Pt etc., even diamond on field emission arrays [1.8-1.10]. Different device schemes also have been proposed to enhance the emission current density, stability, and reliability.

## 1.2 Theory Background of Field Emission

Due to the superior properties of vacuum microelectronic devices, potential applications include high brightness flat-panel display [1.11-1.15], high efficiency microwave amplifier and generator [1.16-1.18], ultra-fast computer, intense electron/ion sources [1.19-1.20], scanning electron microscopy, electron beam lithography, micro-sensor [1.21-1.22], temperature insensitive electronics, and radiation hardness analog and digital circuits

Electron field emission is a quantum mechanical tunneling phenomenon of electrons extracted from the conductive solid surface, such as a metal or a semiconductor, where the surface electric field is extremely high. If a sufficient electric field is applied on the emitter surface, electrons will be emitted through the surface potential barrier into vacuum, even under a very low temperature. In contrast, thermionic emission is the hot electron emission under high temperature and low electric field. Fig. 1-2(a) demonstrates the band diagram of a metal-vacuum system.

Here  $W_0$  is the energy difference between an electron at rest outside the metal and an electron at rest inside the metal, whereas  $W_f$  is the energy difference between the Fermi level and the bottom of the conduction band. The work function  $\phi$  is defined as  $\phi = W_0 - W_f$ . If an external bias is applied, vacuum energy level is reduced and the potential barrier at the surface becomes thinner as shown in Fig. 1-2(b). Then, an electron having energy “W” has a finite probability of passing through the surface barrier. Fowler and Nordheim derive the famous F-N equation (1.1) as follow [1.3]:

$$J = \frac{aE^2}{\phi t^2(y)} \exp[-b\phi^{\frac{3}{2}}v(y)/E], \quad (1-1)$$

Where J is the current density (A/cm<sup>2</sup>). E is the applied electric field (V/cm),  $\phi$  is the work function (in eV),  $a = 1.56 \times 10^{-6}$ ,  $b = -6.831 \times 10^{-7}$ ,  $y = 3.79 \times 10^{-4} \times 10^{-4} E^{1/2} / \phi$ ,  $t^2(y) \sim 1.1$  and  $v(y)$

can be approximated as [1.10]

$$v(y) = \cos(0.5\pi y), \quad (1-2)$$

Or

$$v(y) = 0.95 - y^2. \quad (1-3)$$

Typically, the field emission current  $I$  is measured as a function of the applied voltage  $V$ . Substituting relationships of  $J = I/\alpha$  and  $E = \beta V$  into Eq.(1-1), where  $\alpha$  is the emitting area and  $\beta$  is the local field enhancement factor at the emitting surface, the following equation can be obtained

$$I = \frac{A\alpha\beta^2V^2}{\phi t^2(y)} \exp\left[-bv(y)\frac{\phi^{\frac{3}{2}}}{\beta V}\right]. \quad (1-4)$$

Then taking the log. form of Eq. (1-4) and  $v(y) \sim 1$

$$\log\left(\frac{I}{V^2}\right) = \log\left[1.54 \times 10^{-6} \frac{\alpha\beta^2}{\phi t^2(y)}\right] - 2.97 \times 10^7 \left(\frac{\phi^{\frac{3}{2}}v(y)}{\beta V}\right), \quad (1-5)$$

from Eq. (1-5), the slope of a Fowler-Nordheim (F-N) plot is given by

$$S \equiv slope_{FN} = -2.97 \times 10^7 \left(\frac{\phi^{\frac{3}{2}}}{\beta}\right),$$

(1-6)

The parameter  $\beta$  can be evaluated from the slope  $S$  of the measured F-N plot if the work function  $\phi$  was known

$$\beta = -2.97 \times 10^7 \left(\frac{\phi^{\frac{3}{2}}}{S}\right) \text{ (cm}^{-1}\text{)}, \quad (1-7)$$

The emission area  $\alpha$  can be subsequently extracted from a rearrangement of Eq. (1-5)

$$\alpha = \left(\frac{I}{V^2}\right) \frac{\phi}{1.4 \times 10^{-6} \beta^2} \exp\left(\frac{-9.89}{\sqrt{\phi}}\right) \exp\left(\frac{6.53 \times 10^7 \phi^{\frac{3}{2}}}{\beta V}\right) \text{ (cm}^2\text{)}. \quad (1-8)$$

For example, the electric field at the surface of a spherical emitter of radius  $r$  concentric with

a spherical anode (or gate) of radius  $r+d$  can be represented analytically by

$$E = \frac{V}{r} \left( \frac{r+d}{d} \right), \quad (1-9)$$

Though a realistic electric field in the emitter tip is more complicated than above equation, we can multiple Eq.(1-9) by a geometric factor  $\beta'$  to approximate the real condition.

$$E_{tip} \equiv \text{Function of } (r,d) = \beta' \frac{V}{r} \left( \frac{r+d}{d} \right), \quad (1-10)$$

Where  $r$  is the tip radius of emitter tip,  $d$  is the emitter-anode (gate) distance and  $\beta'$  is a geometric correction factor [1.11].

For a very sharp conical tip emitter, where  $d \gg r$ ,  $E_{tip}$  approaches to  $\beta'(V/r)$ . And for  $r \gg d$ ,  $E_{tip}$  approaches to  $\beta'(V/d)$  which is the solution for a parallel-plate capacitor and for a diode operation in a small anode-to-cathode spacing.

As the gated FEA with very sharp tip radius, Eq. (1-10) can be approximated as:

$$E_{tip} = \beta'(V/r). \quad (1-11)$$

Combining  $E = \beta V$  and Eq. (1-11), we can obtain the relationship:

$$E_{tip} = \beta V = \beta'(V/r), \text{ and } \beta' = \beta r. \quad (1-12)$$

The tip radius  $r$  is usually in the range from a few nm to 50 nm, corresponding to the parameter  $\beta'$  ranging from  $10^{-1}$  to  $10^{-2}$ .

Besides, transconductance  $g_m$  of a field emission device is defined as the change in anode current due to a change in gate voltage [1.2].

$$g_m = \left. \frac{\partial I_c}{\partial V_g} \right|_{V_c}, \quad (1-13)$$

Transconductance of a FED is a figure of merit that gives as an indication of the amount of current charge that can be accomplish by a given change in grid voltage. The transconductance can be increase by using multiple tips or by decreasing the gate-to-cathode spacing for a given anode-to-cathode spacing.

According to the above mention equations (especially Eq.1-5), the following approaches

may therefore be taken to reduce the operating voltage of the field emission devices:

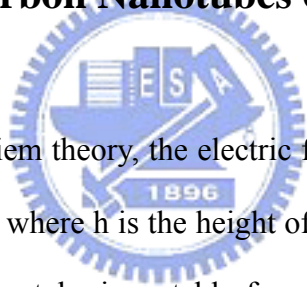
- 1) Find techniques to reproducibly sharpen the tips to the atomic level (increase  $\beta$ ).
- 2) Lower the work function of the tip ( $\phi$ ).
- 3) Narrow the cone angle (increase  $\beta$ ).
- 4) Reduce the gate-opening diameter (increase  $\beta$ ).

### 1.3 Field Emission Properties of Carbon Nanotubes

Recently, carbon nanotubes have attracted considerable attention owing to their unique properties and potential for various applications. The discovery of nanotubes happened in 1991 when Sumio Iijima of NEC Corporation found these tiny needles, consisting of concentric graphite tubes, on the electrodes used to prepare fullerenes [1.23]. Nanotubes can be divided into two categories. The first is called multiwalled carbon nanotubes (MWNTs). MWNTs are close to hollow graphite fibers [1.24], except that they have a much higher degree of structural perfection. They are made of sheets of carbon atoms with a cylindrical shape and generally consist of co-axially arranged 2 to 20 cylinders (Fig. 1-3(b)). The interlayer spacing in MWNT ( $d_{(002)} = 0.34$  nm) is slightly larger than that in single crystal graphite ( $d_{(002)} = 0.335$  nm) [1.25]. This is attributed to a combination of tubule curvature and van der Waals force interactions between successive garphene layers. The second type of the nanotube is made up of just a single layer of carbon atoms. These nanotubes are called the single-walled nanotubes (SWNTs) and possess good uniformity in diameter about 1.2 nm (Fig. 1-3(a)). They are close to fullerenes in size and have a single-layer cylinder extending from end to end [1.26].

These unique structural properties are ascribed to the building material of nanotube---carbon. Carbon is the elemental equivalent of the perfect neighbor, friendly, and easygoing. Under intense pressure, carbon atoms form co-valence bonds with four neighbor atoms, creating the pyramidal arrangement of diamond. However, the activation energy of diamond is very high and carbon usually links up with just three neighbors, creating the hexagonal rings of graphite network. The arrangement of graphite has a host of unpaired electrons, which essentially float above or below the plane of carbon rings. In this arrangement, the electrons have more freedom to move around the graphite surface, which makes the material a good electrical conductor.

## 1.4 Applications of Carbon Nanotubes on Field Emission Display



According to Fowler-Nordheim theory, the electric field at the apex of a needle-shaped tip is enhanced by a factor  $\beta = h/r$ , where  $h$  is the height of the tip and  $r$  is the radius of curvature of the tip apex. The carbon nanotube is a stable form of carbon and can be synthesized by several techniques. They are typically made as threads about 10-100 nm in diameter with a high aspect ratio ( $>1000$ ). These geometric properties, coupled with their high mechanical strength and chemical stability, make carbon nanotubes attractive as electron field emitters. Several groups have recently reported good electron field emission from nanotubes (**shown in figure 1-4**) [1.27-1.28, 1-31].

In 1999, Samsung pronounced a 4.5-inch carbon nanotube based field emission display (**Fig. 1-5**). They mixed a conglomeration of single-walled CNTs into a paste with a nitrocellulose binder and squeezed the concoction through a 20- $\mu\text{m}$  mesh onto a series of metal strips mounted on a glass plate. As the CNTs emerged from the mesh, they were forced into a vertical position. The metal strips with the CNTs sticking out of them served as the

back of the display. The front of the display was a glass plate containing red, green, and blue phosphors and strips of a transparent indium-tin-oxide anode running from side to side. Once assembled, the edges were sealed and air was pumped out of the display. The panel consumes just half the power of an LCD to generate an equivalent level of screen brightness. They could also be cheaper than LCDs or other types of field emission displays being developed.

## **1.5 Other Applications of CNT Emitters**

The range of potential applications for CNT-based field emission is very large. Any system that uses an electron source could potentially host a CNT field emission device. Vacuum electronics would be fast and efficient while providing some definite advantages over solid-state electronics. The electron device of nowadays is based on semiconductor that is sensitive to radiation and high temperature. In contrast, vacuum electronics is insensitive to both. For these reasons, vacuum electronics is still being used in some specific applications (especially military) where improved resistance to temperature variation and high radiation is required [1.1].

### **1.5.1 Vacuum Microelectronics**

Vacuum electronics is based on the controlled propagation of electrons in a vacuum to obtain a signal gain. Miniaturized vacuum electronic devices could overcome the major drawbacks responsible for vacuum tubes. One of the technical advances that may enable future vacuum microelectronics is the possibility of replacing the thermionic emitter found in most classic vacuum tubes by a cold cathode. Because field emitters do not release heat and can be made very small, a miniature field emission cathode could be integrated into a microfabricated vacuum device.



Using carbon nanotubes, high current densities and stable emission have been obtained [1.29], and a gated cathode has been demonstrated [1.30]. Subsequently, this application has driven much of the development of field emitter arrays (FEA), and has reproduced the field of vacuum microelectronics, in which microlithography is used to fabricate FEA cathodes for such amplifier, as well as for flat panel displays.

### **1.5.2. Microwave Amplifiers**

The growth of telecommunication has led to a saturation of the present bands and an increasing demand for new bands at higher frequencies. The use of higher frequencies (10s to 100s of GHz) is, however, limited by the current amplifiers technology. The amplifiers used for high-power microwave transmitters cannot be based on solid-state electronics because conventional transistors are limited by the speed at which charge carriers move through the semiconductor. The basic layout of a traveling wave tube (TWT) is presented in **Figure 1-6**. A thermionic electron source has been typically used in the past to generate the electrons. Cold cathode could replace the thermionic source in TWTs, because field emission offers ultrafast switching capabilities, a triode emitter could be used as an electron buncher in place of the velocity modulator [1.1]. A field emitter capable of producing very high current densities ( $>10\text{A}/\text{cm}^2$ ) could significantly improve the performance of a radio frequency power amplifier tube.

## **1.6 Motivation**

Field emission cathodes with low operation voltage, high emission current, excellent stability and good reliability are aritical to commercialize the field emission devices. However,

CNT has the problem of electron beams, such as the energy spread and beam divergence. Although the emission current is stable in a short-term scale, these nanotube emitters also have a problem of long-term stability which is needed to be overcome especially at high operating voltage. In this thesis, a capping layer was used to improve the reliability of emission current. The lifetime of the device is extended by this method and achieves to a more stable emission current.

According to the F-N equation, to achieve the high emission current at low applied voltage, the work function  $\phi$  of the cathode material must be as low as possible and the field-enhancement factor  $\beta$  and emission area  $\alpha$  should be as large as possible. To obtain a larger  $\beta$ , the conventional method is to produce sharp tips, which required special techniques or complicated fabrication process. For example we can use large oblique-angle thermal evaporation or sputtering to produce sharp metal cones, high temperature oxidation to sharpen silicon tips, or anisotropic etching of silicon using KOH to fabricate sharp tip molds. In this thesis, the capping layer was used to lowering the screening effect of CNTs. Thus, the density of CNTs is decreasing and the field-enhancement factor  $\beta$  is improved by this method. The higher enhancement factor is obtained and may act as the sharp tip and high emission sites. Therefore, the turn-on voltage decreases from 3.6 V/ $\mu\text{m}$  to 2.8 V/ $\mu\text{m}$ , and the field enhancement factor increases from 2960 to 3600.

The field emission devices are roughly divided into two groups: vertical and lateral structure. Lateral type field emission devices have many advantages in high-speed and RF applications owing to simple fabrication, easy control of electrode distances and good electrical characteristics, such as low turn on voltage, high current densities, and high transconductance. However, because of the small micrometer-spacer of the lateral device between the CNT emitter and electrode, the lateral field emission devices have the problem of short circuit. In **figure 1-7** shows the flow chart of conventional lateral device and the short circuit. Thus, a nitride-insulated electrode structure is used in lateral devices to avoid short

current. By this method, the lateral devices have the probability to seal in vacuum. The aligned CNTs and high emission current density are obtained by argon plasma-post-treatment. Superior field emission properties of CNTs, for example, a low turn-on electric field of  $0.8 \text{ V}/\mu\text{m}$  and high emission current density of  $80 \text{ mA}/\text{cm}^2$  have been demonstrated.

## 1.7 Thesis Organization

In chapter 1, the overview of vacuum microelectronics, basic principles of field emission theory and the applications of carbon nanotubes are described.

Chapter 2 reveals the capping layer method to improve the electrical characteristics of carbon nanotubes. A simple method to produce the patterned CNTs using thermal CVD is introduced. Then, the turn-on voltage is decreased and emission current is raised by capping layer. Moreover, the adhesion of CNTs is obviously improved and the reliability is promoted. The synthesis mechanism of CNTs with capping layer is also presumed in this chapter.

In chapter 3, a lateral field emission device is fabricated. Combining semiconductor thin film technology and selective-area growth of CNTs, the lateral field emission CNT diode can be easily obtained. A nitride-insulated electrode structure is used in this chapter to avoid short current. The aligned CNTs and high emission current density are obtained by argon plasma-post-treatment.

Finally, the conclusions and recommendations for future researches are provided in chapters 4.

## Chapter 2

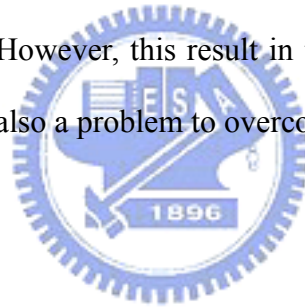
# The Electrical Characteristic Improvement of Carbon Nanotubes by means of Capping Layer Method

In this chapter, we use a capping layer such as Ti to transform the synthesis mechanism of carbon nanotubes (CNTs), and promote the electrical characteristic. The turn-on field decreased from 3.6 V/ $\mu\text{m}$  to 2.8 V/ $\mu\text{m}$ , and can operating at applied field above 7 V/ $\mu\text{m}$  which the emission current is come to 30 mA/ $\text{cm}^2$ . The CNTs is synthesis by thermal chemical vapor deposition (Thermal CVD) and Raman analysis is used to verify the graphite structure and use scanning electron microscope (SEM) to observe the density variation even can know the morphology change of CNTs. The density of CNT decreases from  $10^{10}/\text{cm}^2$  to  $10^8/\text{cm}^2$  by means of capping layer method. Moreover the transmission electron microscope (TEM) not only can validate the multiwall CNTs in this thesis but also helps to figure out even the base growth or tip growth model. Eventually, extracted field emission currents were recorded with a Keithley 237 source-measure unit.

### 2.1 Introduction

Carbon nanotubes (CNTs) are known for their ability to emit a cold electron at relative low voltage [2.1-2.2]. Due to their special physical and chemical characteristic such as superior mechanical strength and low weight [2.3], large surface area useful for adsorption of hydrogen or other gas [2.4]. For vacuum micro-electron device, the superiority of CNTs over

Mo spindt-type field emitter is high aspect ratio, nanometer size tip and high electrical conductivity. Therefore, carbon nanotubes can be applied to field emitters for flat-panel displays [2.5] and vacuum microelectronic devices like microwave power amplifier tubes, field effect transistors (FETs) [2.6], and nano-Schottky diodes. For the synthesis of CNTs, thermal chemical vapor deposition is used in this thesis. However, there also some method to produce CNTs. Arc discharge is the first method to compose of CNTs, which is observed by Iijima in 1991 [2.1]. Arc Discharge can synthesize high purity of CNTs, but it also cost a lot, and the high voltage (above 1000V) operating area may make the process more difficult [2.7, 2.8, 2.9]. Screen-print is used for large-scale area field emission device. One simply harvest CNTs from bulk preparation methods, disperses them in solutions to a known concentration and dip coats them onto a substrate surface [2.10]. This method makes it possible to produce on glass or flexible substrate. However, this result in tangled webs of curly CNTs, and poor adhesion with short lifetime is also a problem to overcome [2.11].



### **2.1.1 Thermal CVD**

In chemical vapor deposition (CVD) process using transition metal particles as reaction catalyst, it is believed that the CNT forms from the saturated metal catalyst surface that resides at either the base [2.12] or the tip of growing nanotubes [2.13-2.14]. In the base growth mode, the CNTs were formed by extraction, resulting in a closed top end. In contrast, in the tip growth mode, a metal catalyst particle remained on the top of each nanotube during growth. The CVD process has many advantages over other deposition methods, including low deposition temperature and control of the diameter of the CNT by varying the size of metal catalyst [2.15]. Furthermore, it is relatively easy to obtain vertically aligned CNTs by increasing nucleation density and growth rate [2.16]. In the CVD process, there are Thermal CVD, plasma enhanced CVD (PECVD) and hot-filament CVD (HFCVD) for nowadays synthesis of CNTs. PECVD and HFCVD by means of the decompositions of carbon and

hydrogen radical by magnetic field or electrical field which can makes CNTs synthesis at low temperature (below 400°C). Low temperature synthesis is a hot issue for CNTs, which makes it possible to use on glass substrate [2.17]. With the control of plasma energy, not only the nucleation sites but also the CNTs density could be adjusted by pretreatment and post-treatment process. However the plasma density and uniformity is hard to control. The run-by-run variation may not be bearable. For the synthesis both single wall and multiwall CNTs, thermal CVD is a convenient technology. The well-accepted growth mechanism of CNTs by thermal CVD involves the decomposition of hydrocarbon gases on the surface of catalyst, the diffusion of carbon into catalyst until saturation, and subsequent segregation of carbon from the catalyst as a tubular structure. These processes are described as the vapor-liquid-solid (VLS) grow model (in figure 2-1) [2.18-2.19]. Numerous researchers report MWCNTs growth by thermal CVD using hydrocarbon (CH<sub>4</sub>, C<sub>2</sub>H<sub>4</sub>, C<sub>2</sub> H<sub>2</sub>, etc.) or Co feedstock and Fe, Ni, or Co as catalysts supported on various substrates [2.24]. The choices for the catalyst, substrate, and the method to transfer the catalyst to the substrate are critical to the success of thermal CVD of nanotubes. Although some paper propose the base growth model when CNTs synthesized by thermal CVD, but the tip growth model is confirm by novel studies and also evidence in this chapter by means of field emission SEM (FE-SEM) and TEM. The field emission property would be hindered by the transition metal, which is on the top of nanotubes. Therefore many groups are trying to remove the tip metal to change the growth model such as ion bombardment in a plasma environment. But it also breaks the graphite structure that for field emission. In our study, we use a capping layer to change the synthesis mechanism to base growth model. Due to this the electrical characteristic can be improvement without destroy the graphite structure.

### 2.1.2 Screening Effect

Nowadays, the diameter distribution and density of CNTs still cannot be controlled

effectively. The screening effects resulting from the dense arrangement of CNTs has been reported by several groups [2.20, 2.21, 2.22]. The density of CNTs at the film surface determines the emission sites density (ESD). If the distance between CNTs is very short, the electric field will be screened out as shown in **figure 2-2**. Groning *et al.* reported that the field enhancement factor  $\beta$  of the tips decreases rapidly when the intertip spacing is smaller than twice the length of the tips. They also found that the maximum current density is obtained when the spacing between the tips is about twice their relative height by simulations, as shown in **figure 2-3**. For larger space, the current density between CNTs decreases as the density of CNTs decrease. With a nearly constant emission current per tip, the field enhancement factor remains constantly. For smaller space, the turn-on field increases rapidly due to the decreasing  $\beta$  factor and this phenomenon cannot be compensated for the quadratic increasing density of the emitting tips. It shows that when the spacing between the emitters on a surface becomes comparable to its length, problems of electric field shielding do occur and may increase the turn-on field dramatically. However, the density of CNTs synthesized by thermal CVD is high for field emission applications. In this chapter, we use a capping layer to suppress the density of CNTs. We can control the CNTs density by means of the different melting point and thickness of the capping layer. Due to the decrease of the screening effect, the turn-on field may be decreased and the emission current may be larger under a suitable capping layer thickness.

### **2.1.3 Adhesion Issue**

Good adhesion between carbon nanotubes and substrate is an essential issue for the applications of CNT-based cold electron emission device. Carbon nanotube has the best field emission property because of nanosize tip, negative work function, good electron conductivity, good thermal conductivity and high aspect ratio. However, CNTs exhibit the worse adhesion properties than carbon nanoparticle or amorphous carbon film. In our experiments, we find

that the CNTs were hard to be well-aligned with poor adhesion between catalyst particles and the substrate as shown in **figure 2-4**. In **figure 2-4(a)**, the catalyst particles fell off from the substrate. In **figure 2-4(b)**, the catalyst rolls up from the substrate. It is not good for CNT-based field emission devices and vacuum electronics. In **figure 2-4(c)**, the catalyst serves to grow another layer of nanotubes above the original aligned CNTs array. It is presumed that the catalyst layer is too thick, so the excess metal-unused served as catalyst at the top of the tower **[2.23]**. Previously, many groups reported that the adhesion of CNTs could be improved by buffer layers such as Ti, Ta, TaN, W. Using the buffer layers not only can improve the adhesion to the substrate but also can decrease the contact resistance between the carbon nanotubes and the substrates. Furthermore, the different compound phases between the substrate and buffer layer are different while CNTs synthesized at high temperature with hydrocarbon feedstock **[2.24]**. The different morphology of CNTs results in buffer layer with different materials. Moreover, with poor adhesion of carbon nanotubes, it is difficult to obtain a stable emission in a macroscopic area of the aligned CNTs array. It is found that the light from the phosphor screen is very unstable **[2.25]**. Therefore, CNTs can be easily pulled off from the substrate resulting in the short-term stability of the emission current. In our experiment, at high applied voltage with long operating time, the degradation of the field emission current can be largely explained for by progressive destruction of CNT structure. This phenomenon may due to the poor adhesion between the CNTs and the substrate. By means of capping layer, the emission current not only can be operated at high electric field (above 12 v/um) without breakdown but also can be stable at long operating time (1hr). The life time of the devices is extended by this method and a more stable emission current is achieved.



## 2.2 Experimental procedures

### 2.2.1 The Preparing of Substrates with Ti Buffer Layer

The multi-wall carbon nanotubes (MWCNTs) were grown on Fe-coated silicon substrate with Ti buffer layer (silicon substrate/Ti buffer layer/Fe catalyst layer) by Thermal CVD process. We used N<sup>+</sup>-type single polished Si (100) wafer with resistivity of 5-10 Ω-cm as our substrate. We used sulfuric acid to remove metal particles and then used HF solution to remove the native oxide from the surface of silicon wafer. These two methods were used to clean the surface of silicon wafers. Then the wafers were patterned by photolithography with spin-coated positive photoresist FH6400 about 2μm. The pattern was 1mmx1mm square with 50x50 small squares in it. Each square was 10μm×10μm with 10μm space to each other. We deposited Ti (50nm) directly by electron beam evaporation system on the patterned Si substrate as a buffer layer between the silicon substrate and CNTs. Then the thin Fe (5nm) layer was deposited as catalyst metal by the same deposition system. Then the Fe patterns are formed after the photoresist is removed by lift-off method as depicted in **figure 2-5 (d)**. And the experimental procedures of CNTs synthesise by capping layer is shown **in figure 2-5**.

### 2.2.2 Thermal CVD process

Before the synthesis of carbon nanotubes, we deposit a capping layer on Fe catalyst particles. First, the Fe catalyst was pre-treated by thermal CVD in H<sub>2</sub> gas environment. The pretreatment environment gas has been considered as a reducing gas for the oxide layer of the catalyst surface [2.26] and also considered as an etching agent or chemical reaction gas to increase the roughness of catalyst. The particle-like catalyst surface is good for the synthesis of carbon nanotubes because of larger area for carbon diffusion. Then we deposit a thin capping layer such as Ti by electron beam evaporation system. By means of H<sub>2</sub> pretreatment

before deposition of capping layer, it makes the reaction surface rougher and also enhances the probability to hydrocarbon radicals to diffuse into the catalyst surface. Eventually, the CNTs were synthesized by thermal CVD system. During CNTs synthesis process, a mixed gas with acetylene (C<sub>2</sub>H<sub>2</sub>), methane (CH<sub>4</sub>), nitrogen (N<sub>2</sub>) and hydrogen (H<sub>2</sub>) was introduced into the thermal CVD chamber as source gases. The temperature of the chamber is rising from room temperature to 700 °C in 11mins and maintaining at 700 °C when the hydrocarbon source is decomposed. The CNTs length and density were affected by growth time, gas flow rate, and also depended on the mixture ratio of reaction feedstock.

### 2.2.3 Material Analysis Instrument

The grown CNTs were observed by HITACHI-S4700 field enhanced scanning electron microscope (FE-SEM) with an energy dispersive X-ray spectrometer (EDX) system. The structure of graphite or defects with SP<sup>3</sup> carbon structure was analyzed by Raman spectrum. The TEM system was also used to check the growth model and the structure of graphite in the CNTs. The photography of TEM, SEM and Raman were shown in [figure 2-6](#).

### 2.2.4 Electric Measurement in a Vacuum System

The sample was measured in a vacuum system ([in figure 2-7](#)). The vacuum chamber is evacuated using a SEIKO SEIKI STP-400 turbo pump. Cathode contact was made directly on the wafer. The anode plate is a glass plate coated with an indium-tin-oxide (ITO) coated glass or a P22 phosphor/ITO/glass screen. The base pressure of the field emission chamber is about  $2.0 \times 10^{-6}$  torr. We measured the samples with anode voltage up to 1000 Volts across the anode and cathode with proper spacing distance. A positive voltage was applied to the anode, and the emission current is measured at the cathode. We use the Keithley 237 with IEEE 488 interface source measurement as high-voltage units (SMU) in our DC measurement. The measurement instruments were auto-controlled by the ICS system. The microscopic electric

field  $E$  was estimated by dividing the applied voltage to the sample-anode separation ( $V/d$ ).

The emission current density  $J$  is calculated from the measured emission current and the area of the CNTs array ( $A/cm^2$ )

## 2.3 Results and Discussion

### 2.3.1 Mechanism

In order to compare the density of CNTs with to without capping layer, here we prepare three samples (a) Ti capping layer (100Å) on  $H_2$  pretreated with Fe catalyst layer (50 Å); (b) Ti capping layer (100 Å) on Fe catalyst layer (50 Å) without  $H_2$  pretreatment; (c)  $H_2$  pretreated Fe catalyst layer (50 Å) without Ti capping layer (see [figure 2-8](#)). The density of CNT obviously decreases with capping layer (shown in [figure 2-8 \(a\)](#) and [figure 2-8 \(b\)](#)). We suppose there are two mechanisms for CNTs synthesis with capping layer. First, the thermionic energy of Ti atoms increased at high temperature and caused the atomic vibration. Although the bulk melting point of Ti is as high as 1668 °C, the Ti atom has the probability to move around the surface. According to Lindemann's criterion, when the thickness of film is decreased to nanometer degree the melting point may be lower to 1/3 and this liquid-like metal may gather together because of cohesion. In terms of the Lindemann's theory, the vibrations among the atoms were called mean-square displacement (MSD) which is rapidly increasing with higher temperature. When the Ti atoms in capping layer move to the Ti buffer layer at high temperature due to the surface energy, the Fe nanoparticles may expose and the carbon radicals can diffuse into the catalyst metal. It is so-called vapor-liquid-solid (VLS) growth model. That is why we need the pretreatment of catalyst surface before depositing the Ti capping layer. The rough surface may cause Ti atoms in capping layer to move to the Ti buffer layer and make a chance for the Fe nanoparticle to be exposed ([shown in figure 2-9\(a\)](#)).

Another synthesis mechanism is that the Fe may not be exposed to the carbon radicals directly. However, the carbon radicals can still overcome the diffusion barrier of very thin Ti layer and diffuse through the thin Ti capping layer and extract the carbon graphite (shown in figure 2-9(b)). The VLS model still could happen when the capping layer is very thin and the carbon atom has high diffusion energy at high temperature to penetrate. Due to this, the carbon nanotubes still can be observed without pretreatment (shown in figure 2-8(b)). So, there are two mechanisms we propose to explain the growth model of CNTs with a very thin Ti capping layer.

### 2.3.2 Thickness Effect of Fe Catalyst in Thermal CVD

The different surface roughness is an important factor for the synthesis of CNTs. Figure 2-10 shows the SEM of Fe 50 Å, 100 Å and 500 Å pretreated in 10 min with H<sub>2</sub> (500 sccm) at 700 °C. The sizes of nanoparticles were about 80 nm, 100 nm and 150 nm. When the catalyst becomes thicker the surface has more non-uniformity as shown in figure 2-10(c). Although the Fe catalyst film with 500 Å has larger roughness, the size of nanoparticles (about 150 nm) is too large to form carbon nanotubes. According to the vapor-liquid-solid (VLS) growth model, the large catalyst surface results in high carbon diffusion velocity. When the diffusion velocity of carbon radicals is faster than the segregating rate of carbon atoms on the surface of catalyst nanoparticles from the liquid interface, it may reach the saturation of deposition of carbon atoms at the surface of catalyst metal and hinder the synthesis mechanism. After capping Ti metal on catalyst with different thickness, no carbon nanotube is observed in Fe 500 Å, (shown in figure 2-11(c)). In general, the diameter of CNT is relative to the catalyst nanoparticles. Thus, the size of catalyst particles should be controlled to 10nm~100nm for the synthesis of CNTs. Thus, we use Fe 50 Å as catalyst in subsequent experiment.

### 2.3.3 Effect of Different Pretreatment Time

The time of pretreatment is also an important factor in the formation of CNTs. **Figure 2-12** shows SEM of different pretreatment time in 5 min, 15min and 30min at 700 °C with H<sub>2</sub> 500 sccm. In growth mechanism of thermal CVD, the H<sub>2</sub> pretreatment is used as reduction agent to remove the oxide from the Fe surface. Unlike the plasma enhancement CVD during pretreatment, we suppose that H<sub>2</sub> decompose at high temperature will not etch the catalyst surface. We presume that the theory of wettability can explain the pretreatment phenomenon in thermal CVD. The wettability of a liquid is defined as the contact angle between a droplet of the liquid in thermal equilibrium on a horizontal surface as illustrated in **figure2-13**. Actually, the wetting angle  $\theta$  is a thermodynamic variable that depends on the interfacial tensions of the surfaces. We suppose that if pretreatment maintains for a very long time (**Fig. 2-12(c)**), the surface energy will be high enough that each Fe nanoparticle may merge together. This phenomenon may result in a smooth catalyst layer and it may hinder the formation of CNTs. Hence, the non-uniformity of Fe nanoparticle may make the diameter of CNTs arrange in disorder. The synthesis of CNTs with different pretreatment time is shown in **figure 2-14**. Due to the good uniformity of Fe nanoparticle with 5 min pretreatment, the diameter of CNTs also distributes uniformly in about 65 nm. From the results of SEM, we choose 5 min as the pretreatment time at 700 °C with H<sub>2</sub> 500 sccm in our experiments.

### 2.3.4 Different Thickness of Ti Capping layer

From the mechanism of CNT formation we mentioned previously, it seems more difficult to grow CNTs with a thick Ti capping layer (shown in **figure 2.15**) Even though the temperature of pretreatment was as high as 700 °C and the Ti atoms can move easily on the surface, the thickness of Ti capping layer on catalyst nanoparticles is still too large for carbon radicals to diffuse through. It is why we can not grow CNTs on catalyst nanoparticles with a thick Ti capping layer. When the carbon graphite extraction rate is slower than the

decomposition of carbon atoms on the surface, amorphous carbon may be formed and no carbon nanotube is observed as shown in **figure 2.15(c)**. Therefore, we choose 50 Å as a proper thickness of Ti capping layer for CNTs formation in our experiments.

### **2.3.5 Density Variation by Different Materials with Different Melting Point**

According to the Lindemann's theory, the moving of Ti atoms on surface is depend on the mean-square displacement (MSD). It also signifies that if the melting point is high, the bonding between two atoms is strong and the migration of atoms is more difficult. Here we anticipate that we can use different materials with melting point to attach different density of CNTs. The assumption is demonstrated in **figure 2-16**. We use Mo, Ti, and Al to vary the density and the melting point of these materials are shown in **table 2-1**. In **figure 2-16**, the capping layer is deposited after hydrogen pretreatment. The melting point of Mo is 2663 °C which is too high for large amount of Mo atoms to move, and maybe the film structure of Mo is too strong for Carbon to diffuse. The carbon can not diffuse through the Mo layer and it also causes the low density of CNTs. However, the density of CNTs with Al capping layer is higher than other capping materials, which may resulting from the lowest melting point (650 °C) of Al in these materials.

### **2.3.6-7-8 Electrical Characteristic Improvements**

#### **2.3.6 The Improvement of Screening Effect**

In the measurement of electrical characteristics, we use three samples (a) H<sub>2</sub> pretreated (for 5 min) Fe catalyst layer (50 Å) with Ti capping layer (50 Å) (b) un-pretreated Fe catalyst layer (50 Å) with Ti capping layer 50 Å (c) H<sub>2</sub> pretreated (for 5mins) Fe catalyst layer (50 Å)

without Ti capping layer (50 Å) (shown in **figure 2-17**). The CNTs were synthesized by thermal CVD at 700 °C for 10 min with the mix of C<sub>2</sub>H<sub>4</sub> 5 sccm and N<sub>2</sub> 500 sccm. Due to the screening effect, it is found that the maximum current density is obtained when the spacing between the tips is about two times of its length. But the emission sites are usually too dense that hinder the emission of electron. By means of capping layer, the density of CNTs decreases obviously and we expect that the turn-on field and current density can be improved. **In figure 2-18(a)**, the turn-on field is decreased from **3.6 v/um to 2.8 v/um** when we use Ti capping layer after catalyst pretreatment. The turn-on field is usually defined as the current density attaining to 10 uA/cm<sup>2</sup>. However, the turn on field of sample (b) is **4.1 v/um** which is even worse than sample (C). This is because the moving of Ti atoms on a smooth surface will not reduce the thickness of Ti capping layer. With hydrogen pretreatment at 700 °C for 5 min, we will get a rough surface with Fe nanoparticles and the Ti buffer layer will appear. The Ti atoms of capping layer will move randomly during the growth of CNTs. We presume that there are two possible ways for Ti atoms to stop at someplace. One is that there are a lot of dangling bonds and defects in the boundary between catalyst nanoparticles and Ti buffer layer and the moving Ti atoms may prefer to stop there. The other is that the surface energy of Ti buffer layers is the same as Ti capping layer and the moving atoms may have chance to merge with the Ti buffer layer. Thus, we use capping layer after hydrogen pretreatment to improve the screening effect. **Figure 2-18(b)** is the F-N plot that shows the field emission characteristics. The field enhancement factor ( $\beta$ ) is also calculated by the slop of the F-N plot. The  $\beta$  is 2960 without capping layer and changes to 3560 when we use Ti capping layer after catalyst pretreatment. The higher enhancement factor obtained maybe due to the presence of defects, which may act as the sharp tip and high emission sites.

The change of growth density and presence of defects were verified by Raman spectroscopy. In **figure 2-19**, spectra of these samples are plotted in the same scale. The nanotubes spectra consist of a graphite peak (G) at ~1590 cm<sup>-1</sup> and a disorder-induced (D)

peak at  $\sim 1350\text{ cm}^{-1}$ . The broad D-band peak is attributed to the disorder-induced features caused by finite size effect in  $\text{sp}^2$  carbon and not an indication of disorder wall structure in the CNTs [2.25]. On the other hand, the broad G-band graphite peak shows the presence of tubular structure in the CNTs [2.26]. **In figure 2-19 (b)** the D-line signal intensity  $I(D)$  is stronger than the G-line graphitic signal intensity  $I(G)$  indicating the synthesized CNTs have a significant amount of defects. The  $I_D/I_G$  changes from 0.71 to 0.9 when the capping layer is deposited after catalyst pretreatment. The defects however are beneficial for promoting the field enhancement factor in field emission. And the intensities of D-peak and G-peak **in figure 2-19 (b)** are relatively lower than **in figure 2-19 (a)**. It also indicates that the density of CNTs with capping layer is much lower than those without Ti capping layer. For the application for field emission device, the emission current density must attain to  $1\text{ mA/cm}^2$ . With our Ti capping layer deposition after catalyst pretreatment, when the current density is  $1\text{ mA/cm}^2$ , the operating voltage arrives at  $3.5\text{ v/um}$  and is better than  $4.5\text{ v/um}$  which is without capping layer.



### 2.3.7 The Improvement of Adhesion Issue

Adhesion is a very critical issue of CNT-based emitters which may result in the problems of reliability and lifetime. Because of the problems of adhesion, the CNTs cannot work at high operating voltage and are difficult to obtain a stable emission current in a macroscopic area at normal operating voltage. With poor adhesion, CNT-based emitters tend to breakdown at high voltage as shown in **figure 2-20**. When the operating electric field up to  $6\text{ v/um}$ , the emission current decreases rapidly. We attribute the degradation of emission current to the decreased effective emission sites of CNTs. After the breakdown phenomenon, the CNTs are pulled off from the substrate and leave holes in the homogeneous aligned CNTs array as shown in **figure 2-20(b)**. Though there are many CNTs remaining on the substrate after breakdown, the nanotubes are almost cut off from the substrate once we magnify the scale at the bottom of



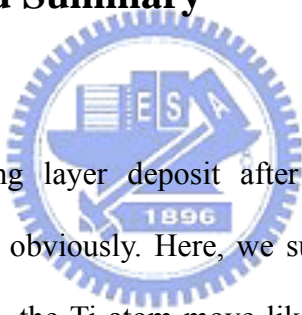
CNT (in figure 2-20(c)). The nanotubes remain on the substrate due to the entanglement by the neighbor CNTs. Therefore, electrons can not transmit through the graphite structure and the field emission characteristics are hindered by those broken CNTs. In figure 2-18(a), we find that with capping layer method, the CNTs can bear high operation voltage operation (above 7 v/um) and the current density is 30 mA/cm<sup>2</sup>. This current level not only can be used for field emission applications but also applied to high power device. With base growth mechanism, the catalyst nanoparticles seem to be fixed on the Ti buffer layer. This phenomenon can improve the adhesion between CNTs and the substrates to prevent some physical damages from static electric force. The capping layer helps the CNTs to stay on the substrate as shown in figure 2-9.

### 2.3.8 The Improvement of Reliability

It is difficult to obtain a stable emission current in a macroscopic area of the aligned CNTs array. Additionally, the long-term stability of the emission current is also a problem. The degradation in the field emission performance can be largely accounted for by progressive destruction between the CNT and the substrate. In figure 2-21(a), at the stress of 10 v/um for 5mins, the CNTs with capping layer have stable emission current density at 6 mA/cm<sup>2</sup>. In contrast, due to the poor adhesion of CNTs, the emission current density degrades rapidly to be less than 1 mA/cm<sup>2</sup> without capping layer. In general, the lifetime of CNT is short, especially at high operating field. The emission current density is less than 0.1 mA/cm<sup>2</sup> after stressing for 1hr in figure 2-21(b). However, without capping layer the CNTs are easily to be pulled off from the substrate and attach to neighbor CNTs. Because the electron transmission is hindered by broken tubes, it may cause the joule heating on the nanotube and even melt down the nanosize tip. Joule heating occurs when a resistor is heated as current flows through it. As shown in figure 2-22, the sharp tips merge together and become smooth. Due to the decrease of aspect ratio, the emission current density is very small and it cannot be

used for field emission display. With our capping layer method, when the CNT array operating at 10 v/um for 1hour, the emission current density decrease from 6 mA/cm<sup>2</sup> to 3 mA/cm<sup>2</sup>, but it still can be applied to field emission display. In figure 2-23, the SEM micrographs of the CNTs which is after and before stress (a) with capping layer and, (b) without capping layer. The photographs of the light emitted by the phosphor screen, which were obtained from a rectangular aligned CNTs array with and without capping layer at 5 v/um(shown in figure 2-24). The images clearly show a homogeneous field emission with capping layer. An increase in electric field caused an increase in the number of emission sites and the image became brighter.

## 2.4 Conclusions and Summary



By means of the capping layer deposit after catalyst pretreatment, the electrical characteristic can be improved obviously. Here, we suppose two mechanisms to synthesize CNTs with capping layer. First, the Ti atom move like liquid and the liquid-like metal may gather together by cohesion. When Ti atoms assemble together like liquid, the Fe may be exposed and fallow the vapor-liquid-solid (VLS) growth model. Second, the Fe may not be exposed but the carbon atoms still can diffuse through the thin Ti capping layer and extract the carbon graphite. The density of CNT decreases from 10<sup>10</sup>/cm<sup>2</sup> to 10<sup>8</sup>/cm<sup>2</sup> by means of capping layer method. Due to the low-density control, the turn on field decreases from 3.6 v/um to 2.8 v/um. Thus, the screening effect is modified by this method and the elevation of emission current attribute to the effective emission sites of CNT. In terms of the capping layer method, the catalyst may fix at the substrate and the CNTs can bear at high operating voltage (above 7 v/um). Therefore, the adhesion of CNT is modified and the current density can attain to 30 mA/cm<sup>2</sup>. Furthermore, long-term stability of the emission current at high operating

voltage can be realized. The photographs of the light emitted by the phosphor screen clearly show a homogeneous field emission current with capping layer. And the optimum condition to synthesize CNTs in thermal CVD is also modified in the thesis.



## Chapter 3

# Fabrication and Characterization of Lateral Field Emission Devices by Nitride-insulated Electrode Structure

In chapter 3, we propose producing a nitride-insulated gate vacuum diode device which is based on carbon nanotubes (CNTs) and the experimental results are reported. We use a nitride-insulated electrode structure to avoid the short current between the CNTs cold cathode and the lateral polysilicon electrode. The distance between polysilicon electrode and the CNTs cathode is determined by the wet etching process. Therefore, the inter-electrode gap is easily formed in good uniformity and reproducibility with dimensions to micrometer degree. Furthermore, this structure makes the lateral diode can be fabricated in vacuum package technology. The CNTs are selectively grown by thermal chemical vapor deposition and the length of CNTs is controlled to about 1 $\mu$ m. Thus, it makes the length of CNTs near the polysilicon electrode. Moreover, a novel process using high density plasma is proposed to modify the morphology of CNTs. Using plasma post-treatment process not only can break the disordered CNTs but also can lessen the length of CNT. The turn-on voltage of the fabricated device with interelectrode gap of 1  $\mu$ m is as low as 2 volt, and the emission current density is as high as 20 A/cm<sup>2</sup> at 18 volt.

### 3.1. Introduction

#### 3.1.1 Vacuum Microelectronics Devices

Vacuum microelectronics is based on the controlled propagation of electrons in a vacuum


to obtain a signal gain.[3.1] Previously, the vacuum tubes suffered from many limitations, all related to the use of thermionic cathode, which typically had to be heated to above 800 °C for electron emission to occur.[3.2] Thus, vacuum tubes only can use for low power device. Furthermore, it may cost more power to heat the cathode than the power needed to operate the tubes. For nowadays applications, solid state transistors and intergrated circuits was used as microwaves power amplifiers (MPA). But solid state transistor also has limitation at operating frequency above gigahertz (GHz). Even there are some new materials such as GaAs, SiGe and SiC attach higher operating frequency. But the process become more complex and it cost a lot. The thermal dissipation at high frequency is also a great issue in solid state device which need to overcome. In contrast, CNTs vacuum device suit for many high power and high frequency applications. This is due to the fundamental speed of electrons in vacuum being about three orders of magnitude faster than in solids. Thanks to the nature of their emission process, directly-density modulation of the electron beam at radio frequencies becomes possible. [3.3] Cold cathode device has low transition time without warm-up and cool down the device. Therefore, CNTs vacuum device are very attractive for field emission displays (FEDs), microwave power amplifiers, scanning tunneling microscopes (STMs), and microsized intense electron sources [3.4-3.7]. Lateral type field emission devices with Si or metal tips have been demonstrated, they have many advantages such as low turn-on voltage, high current densities, and high transconductance. As field emitters, CNTs exhibit excellent field emission characteristics due to their high aspect ratios, small tip radii of curvature, high chemical stability, and high mechanical strength [3.8-3.13]. A low turn-on electric field of 0.8 V/ $\mu\text{m}$  [3.14] and high emission current density of 80mA/cm<sup>2</sup> have been reported [3.15]. In this chapter, the nitride layer was used as hard mask to avoid the short circuit. Thus, the turn-on voltage can be modified by wet etching process changing the spacer between the emitters and electrode. The fabricated device accomplished the low turn-on voltage of 2 volt and extremely high emission current of 0.4 A/cm as the electrode voltage reaches 10 volt.

### 3.1.2 Inductively Coupled Plasma (ICP) Process

Plasma processes are widely used in semiconductor technology. For example, free radicals significantly enhance sputtering deposition, etch, and CVD films stress control processes. For etch process, lower pressure results in longer mean free path, and less collisional scattering, which improve etch profile control. Besides conventional capacitively coupled plasma source cannot generate high density plasma, the ion flux and ion energy of the plasma source are dependently on RF power. It is crucial for a plasma source to be able to control both ion flux and ion energy. Inductively coupled plasma can generate high density plasma at few mTorr with the ability of controlling both ion flux and ion energy.

## 3.2. Experiments

### 3.2.1 Experiment Procedures



Our new lateral vacuum diode was fabricated by deposition three-layer (oxide-polysilicon- silicon nitride) on silicon substrate. The fabrication procedure of the carbon nanotubes lateral field emission device is shown schematically in **figure 3-1(a)-3-1(f)**. First, by the two-steps initial cleaning process, the alkali metal particle and the native oxide has been removed. As shown in Fig. 3(a), the 1 $\mu$ m thermal oxide was grown on a N-type Si (100) substrate at 1050 °C for 3hr. A 200nm-thick poly Si was then deposited on the thermal oxide by low pressure chemical vapor deposition (LPCVD) using pure precursor SiH<sub>4</sub> at 620 °C. The poly Si was further doped with phosphorous using solid diffusion source(PH-1000N) at 950 °C for 25 minutes. The sheet resistance of poly Si was 50  $\Omega$ /cm by 4-point probe. Finally, a 200 nm-thick silicon nitride layer was deposited on poly Si with SiH<sub>2</sub>Cl<sub>2</sub> (105sccm) and NH<sub>3</sub> (35 sccm) mixture at 800 °C for 25mins by low pressure chemical vapor deposition (LPCVD). The film thickness was measured by N-K ellipsometer. Then the wafer was

patterned by photolithography with spin-coated positive photoresist AZ4620 about 8  $\mu\text{m}$ . Here we use thick photoresist film to resist the dry etching process such as plasma bombardment by high density plasma reactive ion etching system (HDP-RIE). In figure 3-1(b) - (c), the nitride-poly-oxide layer that in the backside of wafer was removed by wet etching and dry etching system. Then the silicon nitride layer was etched by the HDP-RIE for 1min. The condition is  $\text{CHF}_3$  40 sccm and Ar 40 sccm with the ICP power 750 W and the bias power 120 W. The poly silicon was then etched at the same system for 1 min. by using  $\text{Cl}_2$  40 sccm  $\text{SF}_6$  10 sccm and  $\text{O}_2$  5 sccm mixture with the ICP power 600 W and the bias power 150 W. The 1  $\mu\text{m}$   $\text{SiO}_2$  layer was continuous etched for 8.5 min by using  $\text{CHF}_3$  40 sccm and Ar 40 sccm with the ICP power 600 W and the bias power 120 W. As shown in **Fig. 3-1(d)** the poly silicon electrode was etched in the wet etching solution of  $\text{HNO}_3$ :  $\text{H}_2\text{O}$ :  $\text{NH}_4\text{F}$  = 64: 33: 3, the distance between polysilicon electrode and the CNTs cathode was controlled by the etching time. Finally, the silicon oxide layer was continuously removed by the wet etching solution of BOE (buffer oxide etcher). Employing the previously patterned photoresist layer as the shadow mask, a thin Fe (5 nm) on Ti buffer layer (50 nm) was deposited directly on the patterned Si substrate as the catalyst metal by electron beam evaporation, and the iron layer was thus formed after the photoresist was removed by the lift-off method as depicted in **Fig.3-1(e)** and **Fig. 3-1(f)**. During CNTs synthesis process, a mixed gas of acetylene ( $\text{C}_2\text{H}_2$ ), methane ( $\text{CH}_4$ ), nitrogen ( $\text{N}_2$ ) and hydrogen ( $\text{H}_2$ ) were introduced into the thermal CVD chamber as source gases. The chamber temperature is rising from room temperature to 700  $^\circ\text{C}$  in 11 min and maintaining at 700  $^\circ\text{C}$  when the hydrocarbon source was decomposition. The CNTs density and length need to be controlled in about 1  $\mu\text{m}$  device hole with mixture ratio of reaction feedstock. The length of CNTs also can modify by high density argon plasma post-treatment and the disordered CNTs is broken at the same time. Here, the CNT was etched by the HDP-RIE for few seconds using Ar 40 sccm with the ICP power 400 W and the bias power 50 W. On the other hand, we could combine the capping metal method address in

chapter 2 and make it possible to control the CNTs density in vacuum diode.

### 3.2.2 Analysis Instrument and Vacuum Measurement System

The growth morphology of CNTs was observed by scanning electron microscopy (SEM) and the field emission properties of lateral-type CNT diodes were measured in a high-vacuum environment with a base pressure of  $3.0 \times 10^{-6}$  Torr. During the measurement, the device was in an emitter grounded configuration with the cathode contact made through the holder to the backside of the Si wafer. The electrode was applied with a voltage swept from -10 V to 10 V to obtain the current-voltage characteristics of the CNT diode. Both the electrode and emitter currents were measured as functions of electrode-to-cathode bias voltage using Keithley 237 high-voltage units with an IEEE 488 interface controlled by a personal computer.



## 3.3. Results and Discussion

### 3.3.1 The Electrical Characteristics Improvement of Lateral Device by Nitride-Insulated Electrode

Compare with conventional vacuum device, it has the advantages of simple process (it only requires one mask) and small structure size. Due to the spacer between emitters and electrode is in micrometer degree, the turn-on voltage is very low and the emission current density is high. However, it also causes the probability of short circuit and the device cannot work when short circuit happens (shown in **figure 3-2(a)**). **Figure 3-2(c)** shows the electrical characteristics of short circuit. Previously, some groups have reported that using wet etching process to etch back the poly electrode could decrease the probability of short circuit. However, some new problems resulted from this method which needed to be overcome: First,



the turn-on voltage and the electrical characteristics would become worse and the short circuit would happen when the length of CNT is still long. Second, the CNTs could be synthesized on the sidewall of oxide insulator when the photoresist is consumed by dry or wet etching system and it also results in short circuit (shown in **figure 3-2(b)**). Therefore, the nitride-insulated electrode structure is used in this chapter (shown in **figure 3-3**). The silicon nitride layer is used as hard mask due to its insensitivity to wet and dry etching system. And silicon nitride layer also has superior mechanical strength. From the figure, the insulated layer avoids the connection between gate and emitters. It successfully solves the short circuit problem by depositing an insulated layer.

The CNTs were selectively grown by thermal CVD with C<sub>2</sub>H<sub>4</sub> (5 sccm) and N<sub>2</sub> (500 sccm) at 700 °C for 8 mins. The average height of the CNTs is about 1.5 μm and the gap between the electrode and CNTs is 1.5 μm. Varying the poly-Si lateral etching time can control the gap between the electrode and emitters. The electrical characteristic of nitride-insulated electrode structure is shown in **figure 3-4(a)**. The turn-on voltage is defined as the electrode current is 10 uA/cm<sup>2</sup>. The turn-on voltage of the fabricated device with interelectrode gap of 1 μm is as low as 2 volt. Low turn-on voltages were achieved by these CNT diodes and the current density attains to 0.4 A/cm<sup>2</sup> when the electrical field comes to 6.5 V/μm. The corresponding F-N plots of the CNT diodes are shown in **figure 3-4(b)**. As shown in **figure 3-4(b)**, nearly straight lines are obtained, indicating the field emission phenomenon of the fabricated lateral CNT device. The field enhancement factor β can be derived from the slope of the F-N plot by assuming a work function of CNTs of 5 eV. The β value is 4.65×10<sup>6</sup> when the electrode-to-emitter gaps of 1 μm.

### 3.3.2 Effect of the Distance between the Anode and the CNTs

In the wet etching system, varying the lateral etching time can control the gaps between the electrode and CNTs. The distance is 1 μm when the etching time of poly-Si is 20 sec as

shown in **figure 3-5(a)**. The etching distance versus etching time is approximating linear and the etching rate is 0.05  $\mu\text{m}$  per second (**in figure 3-5(c)**). The distance can reach as large to 4 $\mu\text{m}$  when the etching time is 90 sec. **Figure 3-5(b)** shows the cross-sectional SEM micrograph when the side etching time is 90 sec. The nitride hard mask has the probability to collapse as long as the spacer is too large. Besides, the turn-on voltage may rise and the electrical characteristics become worse. However, the lateral device may cause short circuit if the spacer is too small.

The CNTs were selectively grown on the catalyst metal within the cathode region. It can be seen that CNTs are uniformly distributed and no carbonaceous particle is observed. **Figure 3-6(a)-(b)** shows a cross-sectional SEM micrograph of the lateral CNT diode. The average height of the CNTs is about 1  $\mu\text{m}$ . The gap between the electrode to CNTs is 1  $\mu\text{m}$  with side etching 20 sec and 2  $\mu\text{m}$  with side etching time 40 sec respectively. **Figure 3-6(c)** indicates emission current-voltage characteristics of lateral-type CNT diode with different electrode-to-emitter gaps. The turn-on voltages ( $V_{\text{on}}$ ) were defined at 0.5 V and 0.2 V with the electrode-to-emitter gaps of 1  $\mu\text{m}$  and 2  $\mu\text{m}$  respectively. Low turn-on voltages were achieved for these CNT diodes. An emission current density of 10  $\text{mA}/\text{cm}^2$  was obtained at the electrode voltages of 6.1 V and 9.2 V for the electrode-to-emitter gaps of 1  $\mu\text{m}$  and 2  $\mu\text{m}$ , respectively. Decreasing the electrode-to-emitter gap can significantly reduce the electrode operation voltage. The corresponding F-N plots of the CNT diodes are shown in the inset of **figure 3-6(c)**. As it can be seen, nearly straight lines are obtained, indicating the field emission phenomenon of the fabricated lateral CNT device. The field enhancement factor  $\beta$  can be derived from the slope of the F-N plot by assuming a work function of CNTs of 5 eV. The  $\beta$  values are  $7.49 \times 10^6 \text{ cm}^{-1}$  and  $3.64 \times 10^6 \text{ cm}^{-1}$  with the electrode-to-emitter gaps of 1  $\mu\text{m}$  and 2  $\mu\text{m}$  respectively. Reducing the anod-to-emitter gap can achieve a larger  $\beta$ , which means a small electrode voltage can create a large  $\beta$  electric field.

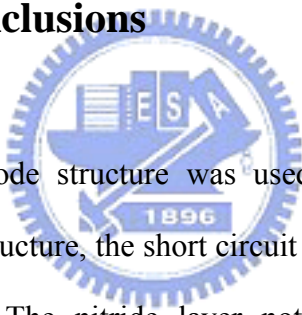
### 3.3.3 Effect of Argon Plasma Post-Treatment

In our previous work, using argon or oxygen high density plasma can modify the morphology of CNTs. The length of CNT decreases as plasma etching time increases. The decreased length results from the destruction of CNTs during plasma treatment. When the reactive neutral species act by themselves such as oxygen plasma, the mechanism is called chemical etching. Because of their incomplete bonding structure, free radicals are highly reactive species. In contrast, ions acting by themselves such as argon plasma can result in physical etching. We expect that the disordered CNTs can be cut off by plasma post-treatment and the short circuit can be avoided [3-16]. In our work, the length of CNTs was as short as 1.5  $\mu\text{m}$ . Thus, the length of CNTs cannot be lessened too much. With short CNTs, the aspect ratio will be decreased and the electrical characteristic will get worse. As a result of this, the chemical etching mechanism may not be used in our experiment. The oxygen plasma not only can remove the disordered CNTs but also destroy the graphite structure in aligned CNTs. The anisotropic etching rate is too fast to be controlled. Here, we use Ar 10 sccm with the ICP power 400 W and the bias power 50 W as etching agent. **Figure 3-7** indicates the SEM micrographs of CNTs treated with different etching times. For the case of 15 sec (**figure 3-7(b)**), the length of CNTs and the density of CNTs were not changed obviously. But the disordered CNTs around the electrode were cut off and also had the probability to remove the catalyst on the tip of CNT. The open tip without catalyst is superior in field emission. For the case of 45 sec (**figure 3-7(d)**), most of the CNTs were destroyed by the plasma. The average length of CNTs was decreased to 0.5  $\mu\text{m}$ . Its field emission characteristics become worse due to high energy and long-time bombardment of CNTs.

The emission characteristics of the CNTs for different plasma post-treatment times are shown in **figure 3-8(a)**. For the post-treatment time 15sec, the turn on voltage decreased from 2 v to 1 v and the current density rose from 0.4 A/cm to 0.6 A/cm. We suppose that the catalyst on the tip of emission site was removed by Ar plasma bombardment. With physical

isotropic etching, the disordered CNTs are cut off without destroying the graphite structure. For the post-treatment time 45 sec, the turn-on voltage increased from 2 v to 10 v and the electrical characteristic became worse. Because of the low aspect ratio and the larger spacer between the emitters and electrode, the electrons are hard to transmit and emit. The corresponding Fowler-Nordheim plots for CNTs with different plasma post-treatment times are depicted in figure 3-8(b). The linearity slope of the plots confirms the field emission phenomena. In this chapter, the plasma post-treatment is not used for modifying the length of CNTs. Therefore, the plasma generation power and the post-treatment time must be modified to 400 W and 15 sec.

### 3.4. Summary and conclusions



A nitride-insulated electrode structure was used in our experiment for lateral field emission device. In this new structure, the short circuit can be suppressed and is beneficial for vacuum package technology. The nitride layer not only uses as hard mask for CNT synthesizing but also has superior mechanical strength in process. The distance between polysilicon electrode and the CNTs emitter was determined by the wet etching process. Thus, the interelectrode gap was easily formed in good uniformity and reproducibility with dimensions about 1  $\mu\text{m}$ . Finally, argon plasma-post-treatment was introduced on the lateral field emission diode to cut off the disordered CNTs and removed the catalyst on the tip of CNTs. And the length of CNTs could be optimized under proper plasma-post-treatment. The turn-on voltage of the fabricated device with interelectrode gap of 1  $\mu\text{m}$  is as low as 2 volt, and the emission current density is as high as 20 A/cm at 18 volt.

## Chapter 4

### Conclusions and Future Prospects

#### 4.1 Conclusions

When carbon nanotubes are synthesized by thermal chemical vapor deposition, the electrical characteristic can be improved obviously by means of using capping layers. Here, the catalyst were pretreated at H<sub>2</sub> environment before capping layer deposition. Thus, particle-like catalyst surface is useful for the synthesis of carbon nanotubes due to a larger carbon diffusion area and the enhancement of the probability of hydrocarbon reaction source to diffuse into the catalyst surface. We suppose two mechanisms to synthesize CNTs with capping layer: (1) When Ti atoms assemble together by cohesion, the Fe may be exposed and follow the vapor-liquid-solid (VLS) growth model. That is why we need pretreatment of catalyst surface before depositing the capping layer. The rough surface may cause Ti atoms to gather to the Ti buffer layer and make a chance for the Fe nanoparticle to be exposed. (2) Another synthesis mechanism is that the Fe may not be exposed but the carbon atoms still can diffuse through the thin Ti capping layer and extract the carbon graphite

The density of CNT decreases obviously by capping layer deposition. The density of CNT decreases from  $10^{10}/\text{cm}^2$  to  $10^8/\text{cm}^2$ . According to the lowering of screening effect, the turn-on field can be decreased from  $3.6 \text{ v}/\mu\text{m}$  to  $2.8 \text{ v}/\mu\text{m}$ . The field enhancement factor  $\beta$  is  $2960$  without capping layer and changes to  $3560$  when we use capping layer method. Moreover, the defects also increase due to the hindering by capping metal when CNT synthesizing. The defects, however, are beneficial for promoting the field enhancement factor in field emission. When the current density is  $1 \text{ mA}/\text{cm}^2$ , the operating voltage arrives at  $3.5$

v/um and is better than 4.5 v/um without capping layer.

The most contributive of capping layer is the adhesion improvement especially at high operating voltage. The catalyst may fix at the substrate; thus, the CNTs can bear at high operation voltage (above 7 v/um) and the current density attains to 30 mA/cm<sup>2</sup>. The long-term stability of the emission current is realized, and after stress at 1000 V in 1hr the homogeneous field emission current is shown from the light emitted by the phosphor screen.

A new fabrication method of CNT nitride-insulated lateral field emission device has been demonstrated. Utilizing semiconductor fabrication technology and selective-area growth of CNTs, CNT lateral field emission diode can be easily obtained. The electrode-to-emitter gap can be reduced about 1 μm by controlling the lateral etching time. In this new structure, the short circuit can be voided and is beneficial for vacuum package technology. The nitride layer not only is used as hard mask for CNT synthesizing but also has superior mechanical strength in process. Moreover, the modification of surface morphology of CNTs has been achieved by post plasma treatments. The field emission characteristics have confirmed the improvement of field emission properties under suitable PPT conditions. Therefore, the length of CNTs and the density of CNTs were not changed obviously, but the disorder CNTs around the electrode is being cut off. The turn-on voltage of the fabricated device with interelectrode gap of 1 μm is as low as 2 volt, and the emission current density is as high as 20 A/cm<sup>2</sup> at 18 volt.

## 4.2 Future Prospects

### 4.2.1 Future Prospects of CNTs Synthesizing with Capping Layer via Thermal CVD

(1) The low density of CNTs is depending on the melting point of capping layer.

(A) We can try another capping material (such as Mo, Al) and analyze the electrical

characteristic

(B) Try the suitable thickness of capping layer that has the optimum density of CNTs.

(2) The adhesion improvement is depending on the alloy phase of capping metal-catalyst-buffer layer

(1) Try different buffer layer (such as Mo, Al, Cr) and analyze the electrical characteristic.

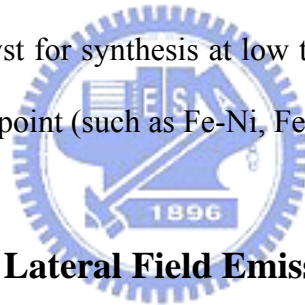
(2) Analyze the compound phase and the alloy component at the bottom of CNTs.

(3) In order to achieve growth on glass substrate, we must try the method for synthesis at low temperature

(1) Synthesized by using MPECVD with capping layer, the growth temperature may be lower.

But the synthesis mechanism must be modified.

(2) By using another catalyst for synthesis at low temperature, especially the alloy which can lower the melting point (such as Fe-Ni, Fe-C, Ni-Pd).



#### **4.2.2 Future Prospects of Lateral Field Emission Device**

(1) Carbon nanotube lateral field emission triode for vacuum microelectronic application.

(2) In-situ vacuum sealed carbon nanotube lateral field emission diode for high frequency circuit applications.

(3) In-situ vacuum sealed carbon nanotube lateral field emission triode for high frequency circuit applications.

(4) Fabrication of CNTs lateral field emission device for high frequency and high power circuit applications.

(5) The focus gate can be applied to the CNT triodes to improve the emission characteristics.